Published in final edited form as:
J Hypertens. 2011 March ; 29(3): 542–552. doi:10.1097/HJH.0b013e328341cedf.

Inhibition of mineralocorticoid receptor is a renoprotective effect of the 3-hydroxy-3-methylglutaryl-coenzyme A reductase inhibitor pitavastatin

Xian Wu Cheng[a,e,f], **Masafumi Kuzuya**[b], **Takeshi Sasaki**[c], **Aiko Inoue**[b], **Lina Hu**[b], **Haizhen Song**[b], **Zhe Huang**[b], **Ping Li**[a], **Kyosuke Takeshita**[a], **Akihiro Hirashiki**[a], **Kohji Sato**[c], **Guo-Ping Shi**[d], **Kenji Okumura**[a,g], and **Toyoaki Murohara**[a]

[a] Department of Cardiology, Nagoya University Graduate School of Medicine, Nagoya

[b] Department of Geriatrics, Nagoya University Graduate School of Medicine, Nagoya

[c] Department of Anatomy and Neuroscience, Hamamatsu University School of Medicine, Hamamatsu, Japan

[d] Department of Cardiovascular Medicine, Brigham and Women's Hospital, Harvard Medical School Boston, Massachusetts, USA

[e] Department of Internal Medicine, Kyung Hee University Hospital, Seoul, Korea

[f] Department of Cardiology, Yanbian University Hospital, Yanji, Jilin Province, China

[g] The Toki Municipal General Hospital, Toki, Gifu Prefecture, Japan

Abstract

Objective—The mineralocorticoid receptor has been implicated in the pathogenesis of chronic cardiorenal disease. Statins improve renal remodeling and dysfunction in patients with proteinuric kidney diseases. We aimed to clarify the beneficial effects and mechanisms of action of statins in renal insufficiency.

Methods and results—Dahl salt-sensitive rats fed a high-salt diet were treated from 12 to 20 weeks of age with vehicle, the reduced nicotinamide-adenine dinucleotide phosphate (NADPH) oxidase inhibitor apocynin, the synthetic cathepsin inhibitor E64d, or a low or high dosage of pitavastatin (1 or 3 mg/kg daily). Rats fed a low-salt diet served as controls. Rats on the high-salt diet developed massive proteinuria and glomerulosclerosis; these changes were attenuated by both doses of pitavastatin. The amounts of mRNAs or proteins for mineralocorticoid receptor, angiotensin-converting enzyme, angiotensin II type 1 receptor (AT1R), monocyte chemoattractant protein-1, osteopontin, macrophage infiltration, and NADPH subunits ($gp91^{phox}$, $p22^{phox}$, and Rac1) were significantly higher in the failing kidneys of vehicle-treated rats than in the kidneys of control rats. Either dose of pitavastatin significantly attenuated these changes. These effects of pitavastatin were mimicked by those of apocynin and E64d. Pretreatment with pitavastatin and apocynin inhibited mRNA and protein of mineralocorticoid receptor induced by angiotensin II in cultured podocytes.

Conclusion—The beneficial effects of pitavastatin are likely attributable, at least in part, to attenuation of the mineralocorticoid receptor-dependent inflammatory mediator, matrix protein,

Correspondence to Xian Wu Cheng, MD, PhD, Department of Cardiology, Nagoya University Graduate School of Medicine, 65 Tsuruma-cho, Showa-ku, Nagoya 466-8550, Japan, Tel: +81 52 744 2150; fax: +81 52 744 2210; chengxw0908@yahoo.com.cn.

There are no conflicts of interest.

and cathepsin expressions induced by AT1R-mediated NADPH oxidase activation in the kidneys of a salt-induced hypertensive Dahl salt-sensitive rat model.

Keywords

hypertension; mineralocorticoid receptor; oxidative stress; renal insufficiency; salt; statin

Introduction

Renin–angiotensin system (RAS) activation has been shown to exert pressor, profibrotic, and proinflammatory actions [1]. The reduced nicotinamide-adenine dinucleotide phosphate (NADPH) oxidase complex is thought to be a major source of the reactive oxygen species (ROS) generated in the cardiorenal system in response to angiotensin II (Ang II) [2–4]. ROS derived from NADPH oxidase activation contribute to the development of hypertension, albuminuria, and progressive glomerular dysfunction, which may ultimately lead to chronic kidney disease (CKD) [5]. Recently, clinical and experimental evidence has shown that tissue-based RAS activation further modulates cell growth, metabolism, and tissue remodeling [6,7].

The mineralocorticoid receptor, a member of the steroid receptor family, plays a major pathophysiological role in the progression of kidney disease [8], and the inhibition of mineralocorticoid receptor signaling considerably reduces proteinuria in patients with CKD [9]. Although several lines of evidence underscore the importance of mineralocorticoid receptor activation by molecules other than its ligand [5,10], the precise mechanisms regulating the transactivation potential of mineralocorticoid receptor remain unknown.

Hypertensive kidney damage is an important cause of end-stage renal disease, and proteinuria is a strong risk factor for the progression of CKD [11]. Clinical studies have shown that proteinuria and CKD are independent risk factors for death and cardiovascular events [12,13]. Numerous recent studies on experimental animals and humans have shown that in addition to angiotensin-converting enzyme (ACE) inhibitors and Ang II receptor blockers, 3-hydroxy-3-methylglutaryl-coenzyme A (HMG-CoA) reductase inhibitors (statins) are effective in preventing glomerular remodeling and ameliorating albuminuria and glomerular dysfunction [14,15]. Statins have been shown to exert pleiotropic actions, including reducing ROS formation and proinflammatory responses [16,17] and regulating the expression of thrombogenesis-related genes [18,19]. The mechanisms by which statins exert these actions remain elusive. Because the inhibition of mineralocorticoid receptor prevents the pathogenesis of multiple cardiorenal diseases [6,20], we speculated that the cardiorenoprotective effects of statins may ameliorate salt-induced hypertensive organ damage and that the actions of statins are linked to regulation of the mineralocorticoid receptor signaling pathway.

The Dahl salt-sensitive rat model constitutes a paradigm of salt-sensitive hypertension in humans and is, therefore, a useful animal model for investigating the mechanism underlying cardiovascular and renal injury in response to hypertension associated with salt intake [3,6,21,22]. To elucidate the renal protective effects of statins, as well as the mechanism of action of these drugs in reducing hypertension-induced local enhancement of mineralocorticoid receptor-dependent inflammatory response and of matrix protein and cathepsin expression, we performed studies using a salt-induced rat hypertension model. Our results provide novel evidence on the cross-talk between mineralocorticoid receptor and Ang II/angiotensin II type 1 receptor (AT1R) signaling in renal remodeling.

Methods

Animals and treatments

Male inbred Dahl salt-sensitive rats were obtained from Eisai (Tokyo, Japan) and handled in accordance with both the revised guidelines of Nagoya University Graduate School of Medicine and the NIH Guide for the Care and Use of Laboratory Animals. Weaned Dahl salt-sensitive rats were fed laboratory chow until 7 weeks of age. Both food and tap water were provided *ad libitum* throughout the experimental period. The rats were fed an 8% NaCl diet (DSH) from 7 weeks of age to induce renal failure, and at 12 weeks of age, they were randomized into three treatment groups (n = 10 in each group): vehicle (0.5% carboxymethylcellulose, DSH+Veh), low dose of pitavastatin (1 mg/kg per day; DSH+Pit-L; Kowa Pharmaceutical Co. Ltd., Nagoya, Japan), and high dose of pitavastatin (3 mg/kg per day; DSH+Pit-H), given by oral gavage every day until 20 weeks of age. Rats fed a low-salt (0.3% NaCl) diet served as age-matched controls (DSL-C, n = 10).

To evaluate whether renoprotection by a statin was linked to a decrease in renal mineralocorticoid receptor expression and a concomitant reduction in NADPH oxidase-derived superoxide production, Dahl salt-sensitive rats that were fed a high-salt diet (n = 6 in each group) were also treated with an NADPH oxidase inhibitor, apocynin (0.5 mmol/kg per day in the drinking water daily, DSH+Apo), or vehicle (DSH+Veh), until 20 weeks of age. To evaluate whether cathepsin activation induced by oxidative stress involves renal remodeling and dysfunction, a synthetic cathepsin inhibitor, E64d (10 mg/kg; Sigma-Aldrich, St Louis, Missouri, USA), dissolved in dimethyl sulfoxide (DMSO, DSH+E64d) or vehicle (DSH+Veh) alone was injected into the abdomens of high-salt-treated Dahl salt-sensitive rats (n = 6 in each group) every other day until 20 weeks of age.

The doses of pitavastatin, apocynin, and E64d were determined according to several previous studies [3,4,23]. At 20 weeks of age, all of the rats were euthanized by intraperitoneal overdose of sodium pentobarbital (50 mg/kg), a blood sample was collected from the abdominal aorta for biochemistry, and the kidneys were harvested for biological and histological analyses.

Urinalysis and systolic blood pressure measurement

Twenty-four-hour urine was collected using a metabolic cage before, during, and near the end of treatment (i.e., at 11, 15, and 19 weeks), and urine albumin levels were determined by pyrogallol assay (MicroTP-AR, Wako, Osaka, Japan). SBP was measured weekly in conscious rats from 7 weeks of age by tail-cuff plethysmography (BP-98A; Softron, Tokyo, Japan) [3].

Histology and immunohistochemistry

Kidneys were fixed in ice-cold 4% paraformaldehyde solution for 24 h, embedded in paraffin, and processed for histology and immunohistochemistry as described previously [3]. Renal transverse tissue sections (3 μm) were stained with hematoxylin–eosin solution for routine histological examination; Azan-Mallory solution (Muto Pure Chemicals Co., Ltd., Tokyo, Japan) was used to evaluate glomerular and perivascular fibrosis [23], and periodic acid-Schiff solution (Muto) was used to evaluate glomerulosclerosis and tubulointerstitial injury [22]. The glomerulosclerosis index was semiquantitatively calculated through the examination of 20 glomeruli from four independent sections of each animal (n = 6 per group) and graded from 0 to 4+. Tubulointerstitial injury was scored as 0 (0%), 1+ (1–10%), 2+ (11–25%), 3+ (26–50%), 4+ (51–75%), or 5+ (76–100%) in accordance with a scoring system reported previously [5]. Glomerular fibrosis was analyzed in 20 glomeruli from four independent sections of each animal (n = 6 per group) and was expressed as the area stained

per glomerulus. Perivascular fibrosis was analyzed in the perivascular regions and expressed as the stained area per fixed quantification area (mm^2).

For immunohistochemistry, sections were stained with a mouse monoclonal antibody (mAb) to rat CD68 (clone ED1; Chemicon, Temecula, California, USA) to visualize macrophages, or with an antihuman mineralocorticoid receptor mouse mAb (clone H3122; Perseus Proteomics, Tokyo, Japan) [4]. Macrophages that infiltrated the glomeruli and perivascular regions were counted in four random microscopic fields from three independent sections of each animal ($n = 6$), and the infiltration was expressed as the number of macrophages per glomerulus or fixed perivascular quantification area (mm^2) (400 ×). For immunofluorescence, sections were treated with a mouse mAb against human desmin (Clone D33; Dako, Glostrup, Denmark) and visualized with a fluorescein isothiocyanate (FITC)-conjugated antimouse immunoglobulin (Ig) G (Medical & Biological Laboratories Co., Ltd., Nagoya, Japan). Glomerular desmin staining was graded as follows: a signaling area of 0% in the glomerular capillary tuft, 0 (0%); +1 (1–25%), +2 (26–50%), +3 (51–75%), and +4 (76–100%). Staining was analyzed in 20 glomeruli from four independent sections of each animal ($n = 6$). For negative controls, primary antibodies were replaced with nonimmune IgG. All morphometric measurements were performed with WinROOF version 5.0 image-processing software (Mitani, Tokyo, Japan) by two observers.

Quantitative gene expression assay

RNA was harvested from tissue with an RNeasy Fibrous Tissue Mini-Kit and from cultured cells with an RNeasy Micro Kit (Qiagen, Valencia, California, USA) in accordance with the manufacturer's instructions. The mRNA was reverse-transcribed to cDNA with an RNA PCR Core kit (Applied Biosystems, Foster City, California, USA). Quantitative real-time gene expression was studied by using the ABI 7300 Real-Time PCR System (California, USA) with TaqMan Universal PCR Master Mix (Applied Biosystems) using the following conditions: 50°C (2 min) for uracil-N-glycosylase incubation, 94°C (10 min) for AmpliTaq Gold activation, 95°C (15 s), and 59°C (1 min) for 40 cycles. Specific primers and TaqMan probe mixtures for rat-targeted genes of the monocyte chemoattractant protein (MCP-1), osteopontin, collagens (types I and III), mineralocorticoid receptor, and ACE were purchased from AB Applied Biosystems (Assay IDs: Rn01456716_g1, Rn01449972_m1, Rn01526721_m1, Rn01437681_ml, Rn00565562_m1, and Rn00561094_m1, respectively). The levels mineralocorticoid receptor mRNA in cultured podocytes stimulated with Ang II were also analyzed by real-time PCR. Specific primers and probes for genes of the cathepsin family (cathepsins S, K, B and L), cystatin C, $p47^{phox}$, $p67^{phox}$, AT1R for rats were described previously [3,6]. All experiments were performed in triplicate. Transcription of targeted genes was normalized to that of the gene for glyceraldehyde 3-phosphate dehydrogenase (GAPDH).

Western blot analysis

Following the isolation of membranes and nuclear protein fractions from kidney tissues, equal amounts of protein (80 μg/lane) were fractionated by 12% sodium dodecyl sulfate-polyacrylamide gel electrophoresis, and separated proteins were transferred to a polyvinylidene difluoride membrane (Amersham Pharmacia Biotech, Buckinghamshire, UK). The membranes were probed with antibodies to $p22^{phox}$, $p47^{phox}$ (1 : 1000 dilutions; all three were from Santa Cruz Biotechnology, Santa Cruz, California, USA), $gp91^{phox}$ (1 : 1000 dilution; BD Transduction Laboratories, Lexington, Kentucky, USA), Rac1 (1 : 1000 dilution; Millipore, Billerica, Massachusetts, USA), and mineralocorticoid receptor (1 : 1000 dilution; Perseus Proteomics Inc.). Antibodies to GAPDH (1 : 1000 dilution; Santa Cruz Biotechnology) or cyclic AMP response element-binding protein (CREB) (1 : 1000 dilution; Millipore) were used to confirm the equal loading of samples.

Assay of nicotinamide-adenine dinucleotide phosphate oxidase activity and superoxide production

NADPH oxidase activity was measured by lucigenin-based enhanced chemiluminescence assay, as described previously [3]. In brief, a low lucigenin concentration (5 μmol/l) was used to minimize artifactual O_2^- production attributable to redox cycling. One milligram of homogenate protein diluted in 1 ml lysis buffer (in mmol/l: Tris·HCl 20, NaCl 150, EDTA 1, ethylene-glycol-etherdiaminetetra-acetic acid (EGTA 1), and 1% Triton X-100; pH 7.5) was transferred to an assay tube, and NADPH and dark-adapted lucigenin were added to final concentrations of 100 and 5 μmol/l, respectively, immediately before the measurement of chemiluminescence. The chemiluminescence signal was sampled every minute for 12 min with a tube luminometer (20/20; Turner Designs, Sunnyvale, California, USA), and the respective background counts were subtracted from the experimental values.

Transmission electron microscopy

Kidney cortical tissue was thinly sliced, placed immediately in primary electron microscopy fixative, and prepared as described previously [22]. A JEM-1400EX transmission electron microscope (JEOL Ltd., Tokyo, Japan) was used to view all renal samples (at magnifications of 6000 and 60 000).

Biochemical analysis

The levels of aldosterone in the kidney tissues were measured with an APAC-S Aldosterone kit (TFB, Tokyo, Japan) by radioimmunoassay. The levels of corticosterone in kidney tissues were measured with a Rat Corticosterone [^{131}I]Biotrak Assay System (Amersham Biosciences Inc., Piscataway, New Jersey, USA). Plasma levels of tumor necrosis factor (TNF)-α and interleukin (IL)-1β were measured with commercially available kits. All assays were performed in triplicate.

Cell culture and stimulation

The podocytes were cultured in 25-cm^2 flasks (BD Falcon, Franklin Lakes, New Jersey, USA) in RPMI medium 1640 (Invitrogen, Paisley, UK) with added penicillin, streptomycin, insulin, transferrin, selenite (Sigma-Aldrich), and fetal calf serum. The podocyte cells were seeded in 12-well plates (5×10^4/well) in serum-free RPMI 1640 medium overnight. The cells were pre-treated with and without pitavastatin and apocynin for 30 min at the indicated concentrations, and then were cultured in the presence or absence of Ang II (10^{-8} mol/l, Sigma-Aldrich) for 24 h, and the extracts were subjected to quantitative real-time PCR, western blotting, and immunofluorescence.

Immunocytofluorescence

Immunocytofluorescence was performed as described previously [3]. Briefly, podocytes (2×10^4/ml) were plated on coverslips coated with type I collagen and cultured in serum-free RPMI overnight. Following preincubation in the presence or absence of pitavastatin at the indicated concentrations for 30 min, the podocytes were treated with Ang II (10^{-8} mol/l), or left untreated, in serum-free RPMI for 24 h and fixed in 8% paraformaldehyde in phosphate-buffered saline. Following blocking, the cells were treated with an antihuman mineralocorticoid receptor mAb (1 : 100), washed, and then visualized with FITC-conjugated antimouse IgG (1 : 400; Medical & Biological Laboratories, Nagoya, Japan) with confocal microscopy (Olympus Fluoview, Tokyo, Japan). For the negative control, the primary antibody was replaced with nonimmune immunoglobulin G.

Statistical analysis

Data are expressed as means ± SEM. Student's *t*-tests (for comparison between two groups) or one-way analysis of variance (ANOVA; for comparisons of three or more groups) followed by Tukey post-hoc tests were used for statistical analyses. Histological data were analyzed using nonparametric analysis with Kruskal–Wallis test, followed by Mann–Whitney *U* test. The data of urine volume and urinary albumin were subjected to two-way repeated measures ANOVA and Bonferroni's post-hoc tests. SPSS software version 17.0 (SPSS Inc., Chicago, Illinois, USA) was used. A value of *P* less than 0.05 was considered statistically significant. All of the morphometric measurements were performed by two observers in a blind manner, and the values they obtained were averaged.

Results

Dahl salt-sensitive rats fed a high-salt diet from 7 weeks of age progressively developed hypertension. Blood pressure (BP) was significantly higher in animals on the high-salt diet (DSH+Veh) than in those on the 0.3% NaCl diet (DSL-C) at 20 weeks of age (237 ± 4 vs. 121 ± 2 mmHg, $P < 0.05$). Either dose of pitavastatin reduced BP without a significant difference (227 ± 54 and 228 ± 4 mmHg, respectively, $P > 0.05$).

Temporal profile of urine volume and urinary albumin

Urine volumes and urinary albumin were measured in all rats at 11, 15, and 19 weeks of age. Urine volume was significantly greater in DSH+Veh rats than in DSL-C rats at 19 weeks of age only ($P < 0.05$, Fig. 1a). However, urinary albumin was significantly higher in DSH +Veh rats than in control rats at all time points ($P < 0.05$, Fig. 1b); these changes were improved by Pit-L or PitH at 15 and 19 weeks of age.

Pitavastatin prevents podocyte and glomerular injury

Immunofluorescence showed that signals were not detected in the glomeruli of the DSL-C rats (Fig. 1c). By contrast, multiple glomeruli were positive for desmin along the capillary tufts in DSH+Veh rats. This effect was confirmed by quantitative analysis of the desmin signaling area (Fig. 1d). TEM showed that pitavastatin prevented podocyte foot-process effacement (Fig. 2a, b). Periodic acid-Schiff staining showed that DSH+Veh rats exhibited severe focal-segmental or global glomerulosclerosis, together with interstitial fibrosis and tubular cast formation (Fig. 2c). The glomerulosclerosis index and tubulointerstitial injury score, together with the areas of glomerular and perivascular fibrosis analyzed by Azan-Mallory staining, were significantly greater in DSH+Veh rats than in control rats (Fig. 2d, e; Fig. 3a–c). These effects were also attenuated by Pit-L and Pit-H.

Effect of pitavastatin on the local levels of hormones and mineralocorticoid receptor, angiotensin II type 1 receptor, and angiotensin-converting enzyme mRNAs

Radioimmunoassay revealed that the levels of aldosterone were significantly lower in the kidneys of DSH+ Veh rats than in those of DSL-C rats (448 ± 77 vs. 173 ± 27 pg/mg, $P < 0.05$), and this change was not significantly decreased in DSH+Pit-L and DSH+Pit-H rats (159 ± 44 and 148 ± 56 pg/mg, respectively, $P > 0.05$). However, there were no significant differences in the levels of corticosterone among the four groups ($P > 0.05$, data not shown). Immunostaining showed that mineralocorticoid receptor was localized predominantly in glomerular cells and tubular cells (Fig. 3d). The data from quantitative PCR and western blotting analysis revealed that the levels of mineralocorticoid receptor mRNA and protein were higher in DSH+Veh rats than in DSL-C rats (Fig. 3e, f). Pit-L and Pit-H both ameliorated these changes (Fig. 3d–f). Similarly, the amounts of ACE and AT1R mRNAs

were higher in the DSH+Veh rats than in the DSL-C rats, and these changes were reduced by Pit-L and Pit-H (Table 1).

Pitavastatin attenuates nicotinamide-adenine dinucleotide phosphate oxidase–derived superoxide production and expression of nicotinamide-adenine dinucleotide phosphate oxidase subunits

Quantitative enzyme assay revealed that NADPH activity in the renal tissue was significantly increased in DSH+Veh rats, and this increase was attenuated in Pit-L and Pit-H rats (Fig. 4a). By western blot assays and PCR assays, we confirmed that the amounts of NADPH oxidase subunit proteins ($p22^{phox}$, $gp91^{phox}$, and Rac-1) and mRNA transcript levels for $p47^{phox}$ and $p67^{phox}$ were significantly increased in DSH+Veh rats, and that these increases were attenuated in DSH+Pit-L and DSH+Pit-H rats (Fig. 4b–d).

Effects of pitavastatin on inflammation actions and on collagen and cathepsin gene expression

Quantitative analysis confirmed that the number of macrophages was significantly higher in the glomeruli and the perivascular region of DSH+Veh rats than in those of DSL-C rats (Fig. 5a–c). This accumulation was accompanied by significant increases in the abundance of MCP-1 mRNA and osteopontin mRNA in the kidneys and significant increases in the plasma levels of TNF-α and IL-1β (Table 1). These inflammatory actions were attenuated by pitavastatin. Similarly, collagen types I and III were significantly higher in the kidneys of DSH+Veh rats than in those of controls, and both Pit-L and Pit-H attenuated these effects (Table 1). PCR analysis revealed that the abundance of cathepsins S, B, and L and of cystatin C was significantly greater (510, 200, 230, 190%, respectively) in the kidneys of DSH+Veh rats than in those of controls; these effects were attenuated by Pit-L and Pit-H (Table 1). However, there was no significant difference in the cathepsin K gene among the four experimental groups.

Effects of apocynin and E64d on mineralocorticoid receptor protein or/and glomerulosclerosis and albuminuria

As shown in Fig. 6a–c, the administration of the NADPH oxidase inhibitor apocynin lessened not only mineralocorticoid receptor protein expression but also the glomerulosclerosis index and albuminuria. Cathepsin inhibitor E64d attenuated albuminuria and glomerular and perivascular fibrosis (Fig. 6d–f).

Pitavastatin inhibits angiotensin II–induced mineralocorticoid receptor expression in cultured rat podocytes

The abundance of mineralocorticoid receptor mRNA in cultured rat podocytes was significantly increased in a dose-dependent manner by exposure to Ang II, and this effect was significantly inhibited by pitavastatin at several concentrations (Fig. 7a, b). Without Ang II treatment, weak immunofluorescence signals were distributed mainly in the cytoplasm of podocytes. A strong staining signal promptly became visible in the nuclei of podocytes stimulated by Ang II; this signal was inhibited by pitavastatin or apocynin (Fig. 7c). Consistent with these results, western blot analysis showed that the exposure of podocytes to Ang II also induced a significant increase in the mineralocorticoid receptor protein level; this increase was inhibited by pitavastatin or apocynin, whereas a combination treatment had no additive effect (Fig. 7d).

Discussion

Several important observations can be made on the basis of these results. First, the administration of pitavastatin to Dahl salt-sensitive rats ameliorated glomerular remodeling and dysfunction in failing kidneys, concomitant with decreases in mineralocorticoid receptor gene expression and protein production, AT1R gene expression, O_2^- generation, inflammatory actions, and cathepsin gene expression. Second, the inhibition of NADPH oxidase activity by apocynin significantly reduced mineralocorticoid receptor expression as well as glomerular remodeling in the failing kidneys of Dahl salt-sensitive rats. Third, selective inhibition of cathepsins by E64d also attenuated glomerular and perivascular fibrosis, as well as proteinuria, in hypertensive Dahl salt-sensitive rats. Finally, the Ang II signal cascade enhanced mineralocorticoid receptor expression in cultured podocytes via NADPH oxidase activation.

Dahl salt-sensitive rats on a high-salt diet showed an increase in mineralocorticoid receptor expression in conjunction with podocyte injury/effacement and the loss of slit-pore diaphragm integrity; these changes were prevented by pitavastatin. Mineralocorticoid receptor expression was accompanied by upregulation of desmin, a protein necessary for the maintenance of podocyte slit-pore diaphragm integrity [20]. This protein upregulation in turn contributed to the effacement of podocytes and the loss of integrity of the slit-pore diaphragm, which are both prerequisites for the progression of albuminuria [24]. Pit-L and Pit-H both reduced the proteinuria that accompanied these podocyte injury markers in hypertensive Dahl salt-sensitive rats, suggesting that the pitavastatin-mediated improvement of renal insufficiency was attributable to its prevention of the injury in the podocyte and glomerular filtration barrier associated with mineralocorticoid receptor upregulation. It is noteworthy that both doses of pitavastatin had no significant effect on the BP. Recent studies using the same model have reported that statins exhibit neither antihypertensive effects nor their natural lipid-lowering ability [23,25]. Taken together, these results suggest that the pitavastatin-mediated beneficial effect in the DSH rats is attributable not to the lipid-lowering and hypertension-lowering effect but to a pleiotropic effect.

Previous studies reported that the levels of ACE and AT1R mRNAs were upregulated in the failing myocardium of Dahl salt-sensitive rats [3,4]. Similarly, our observations have shown that the levels of these genes are increased in the failing kidney tissues of Dahl salt-sensitive rats; these effects were attenuated by pitavastatin. Furthermore, radioimmunoassay showed that the level of aldosterone was decreased more in the kidneys of DSH+Veh rats than in those of DSL-C rats, and this change was not affected by pitavastatin treatment. Taken together, the results suggest that, in this model, the inhibitory effect of pitavastatin on renal injury can be attributed more to the role of this statin in inhibiting Ang II/AT1R signaling pathway activation than to its role in further reducing the impairment of aldosterone synthesis.

What are the pathological stimuli for mineralocorticoid receptor transcriptional activity in the kidneys of DSH rats? It is well established that NADPH oxidase is a major source of ROS generated in the cardiovascular and renal systems in response to Ang II. Ang II stimulates gene transcription via functional mineralocorticoid receptor in cultured human coronary smooth muscle cells independently of aldosterone generation [26]. We have here observed that the administration of NADPH oxidase inhibitor apocynin lessened the proteinuria and glomerular remodeling and mineralocorticoid receptor protein production in kidney tissues. In podocyte cells, pretreatment with apocynin reduced Ang II-induced mineralocorticoid receptor protein production. On the basis of these findings, we propose that an Ang II-mediated NADPH oxidase activation signaling pathway may be responsible for the stimulation of mineralocorticoid receptor transcriptional activity. Additionally, our

observations showed that pitavastatin not only effectively attenuated mineralocorticoid receptor expression and NADPH oxidase activity and its subunit expressions (mRNAs for $p47^{phox}$, $p67^{phox}$, proteins for $gp91^{phox}$, $p22^{phox}$, Rac1) but also ameliorated the proteinuria and glomerular remodeling in the kidneys of DSH rats. It has been previously reported that enhanced mineralocorticoid receptor signaling plays a critical role in the development of podocyte damage and glomerulosclerosis in this low-aldosterone model [22]. Taken together, these findings suggest that mineralocorticoid receptor upregulation subsequent to NADPH oxidase activation depends in part on an Ang II-mediated signaling pathway and represents a target for statin therapy.

Macrophage infiltration of the glomeruli and perivascular spaces of intramural renal vessels was accompanied by increases in the plasma levels of the inflammatory cytokines TNF-α and IL-1β, as well as increased expression of the genes encoding MCP-1 and osteopontin, in the failing kidney tissues of DSH rats. That these effects were sensitive to pitavastatin suggests that the inflammatory responses induced by the mineralocorticoid receptor signaling pathway contribute to the glomerular injury and fibrosis apparent in this model. Osteopontin and MCP-1 play important roles in the development of heart failure in various animal models [4,27]. Thus, the pitavastatin-mediated inhibition of inflammatory action induced by a reduction in mineralocorticoid receptor expression may contribute to the attenuation of renal remodeling in Dahl salt-sensitive rats on high-salt diet, thereby leading to the improvement of kidney function.

The inhibition of cathepsin improves cardiac diastolic function and attenuates cardiac fibrosis in Dahl salt-sensitive rats with heart failure [3]. Our results here demonstrated for the first time that the suppression of cathepsin activity by E64d attenuated glomerular and perivascular fibrosis and proteinuria in the failing kidneys of Dahl salt-sensitive rats. We further revealed that pitavastatin reduced the expression of matrix proteins (type I and III collagens) and cathepsins (including cathepsins S, B, L, and cystatin C) genes in the kidney tissues of DSH+Veh rats. NADPH oxidase-dependent oxidative stress stimulates cathepsin expression and activity *in vivo* and *in vitro* [3,4]. These findings suggested that the renal protective actions of statins are also likely attributable, at least in part, to the attenuation of cathepsin activation and extracellular matrix degradation associated with NADPH oxidase activation.

Clinical implications

We have shown that pitavastatin attenuates the development of renal failure and prevents glomerular filtration barrier injury and subsequent proteinuria in low-aldosterone hypertensive rats. Our findings provide evidence that there is cross-talk between mineralocorticoid receptor and Ang II/AT1R/signaling in nonepithelial kidney cells. The beneficial effects of pitavastatin are likely attributable, at least in part, to attenuation of the renal mineralocorticoid receptor expression stimulated by AT1R-mediated NADPH oxidase activation. Statins may, thus, be of wide therapeutic potential in various cardiorenal diseases, with benefits not limited to those characterized by their lipid-lowering effects. However, future studies on humans and on animal models with CKD will be necessary to compare the potential renal benefits of statin monotherapy and of combinations of statins and mineralocorticoid receptor antagonists.

Acknowledgments

We thank Yoshikazu Fujita (Division of Medical Research Engineering) for technical assistance.

The present work was supported in part by grants from the Ministry of Education, Culture, Sports, Science and Technology of Japan (nos. 19590812 and 21590952 to X.W.C.). This work was also supported in part by grants

from the National Natural Science Foundation of China (no.30960128 to X.W.C.) and NIH grants HL60942, HL81090, and HL88547 (G.P.S.) and American Heart Association EIA award 0840118N (G.P.S.).

Pitavastatin was donated by Kowa Pharmaceutical Co. Ltd. (Nagoya, Japan).

Abbreviations

ACE	angiotensin-converting enzyme
Ang II	angiotensin II
AT1R	angiotensin II type 1 receptor
CKD	chronic kidney disease
DMSO	dimethyl sulfoxide
GAPDH	glyceraldehyde-3-phosphate dehydrogenase
HMG-CoA	3-hydroxy-3-methylglutaryl-coenzyme A
IL-1β	interleukin-1 beta
MCP-1	monocyte chemoattractant protein-1
NADPH	nicotinamide-adenine dinucleotide phosphate
RAS	renin–angiotensin system
ROS	reactive oxygen species
TNF-α	tumor necrosis factor alpha

References

1. Sowers JR. Hypertension, angiotensin II, and oxidative stress. N Engl J Med. 2002; 346:1999–2001. [PubMed: 12075063]
2. Doerries C, Grote K, Hilfiker-Kleiner D, Luchtefeld M, Schaefer A, Holland SM, et al. Critical role of the NAD(P)H oxidase subunit p47phox for left ventricular remodeling/dysfunction and survival after myocardial infarction. Circ Res. 2007; 100:894–903. [PubMed: 17332431]
3. Cheng XW, Murohara T, Kuzuya M, Izawa H, Sasaki T, Obata K, et al. Superoxide-dependent cathepsin activation is associated with hypertensive myocardial remodeling and represents a target for angiotensin II type 1 receptor blocker treatment. Am J Pathol. 2008; 173:358–369. [PubMed: 18583318]
4. Cheng XW, Okumura K, Kuzuya M, Jin Z, Nagata K, Obata K, et al. Mechanism of diastolic stiffening of the failing myocardium and its prevention by angiotensin receptor and calcium channel blockers. J Cardiovasc Pharmacol. 2009; 54:47–56. [PubMed: 19528815]
5. Shibata S, Nagase M, Yoshida S, Kawachi H, Fujita T. Podocyte as the target for aldosterone: roles of oxidative stress and Sgk1. Hypertension. 2007; 49:355–364. [PubMed: 17200434]
6. Nagata K, Obata K, Xu J, Ichihara S, Noda A, Kimata H, Kato T. Mineralocorticoid receptor antagonism attenuates cardiac hypertrophy and failure in low-aldosterone hypertensive rats. Hypertension. 2006; 47:656–664. [PubMed: 16505208]
7. Sadoshima J, Izumo S. Molecular characterization of angiotensin II-induced hypertrophy of cardiac myocytes and hyperplasia of cardiac fibroblasts. Critical role of the AT1 receptor subtype. Circ Res. 1993; 73:413–423. [PubMed: 8348686]
8. Le Menuet D, Isnard R, Bichara M, Viengchareun S, Muffat-Joly M, Walker F, et al. Alteration of cardiac and renal functions in transgenic mice overexpressing human mineralocorticoid receptor. J Biol Chem. 2001; 276:38911–38920. [PubMed: 11495902]
9. Chrysostomou A, Becker G. Spironolactone in addition to ACE inhibition to reduce proteinuria in patients with chronic renal disease. N Engl J Med. 2001; 345:925–926. [PubMed: 11565535]

10. Massaad C, Houard N, Lombes M, Barouki R. Modulation of human mineralocorticoid receptor function by protein kinase A. Mol Endocrinol. 1999; 13:57–65. [PubMed: 9892012]
11. Remuzzi G, Bertani T. Pathophysiology of progressive nephropathies. N Engl J Med. 1998; 339:1448–1456. [PubMed: 9811921]
12. Go AS, Chertow GM, Fan D, McCulloch CE, Hsu CY. Chronic kidney disease and the risks of death, cardiovascular events, and hospitalization. N Engl J Med. 2004; 351:1296–1305. [PubMed: 15385656]
13. Kannel WB, Stampfer MJ, Castelli WP, Verter J. The prognostic significance of proteinuria: the Framingham study. Am Heart J. 1984; 108:1347–1352. [PubMed: 6496291]
14. Nakamura T, Sugaya T, Kawagoe Y, Suzuki T, Inoue T, Node K. Effect of pitavastatin on urinary liver-type fatty-acid-binding protein in patients with nondiabetic mild chronic kidney disease. Am J Nephrol. 2006; 26:82–86. [PubMed: 16534182]
15. Yagi S, Aihara K, Ikeda Y, Sumitomo Y, Yoshida S, Ise T, et al. Pitavastatin, an HMG-CoA reductase inhibitor, exerts eNOS-independent protective actions against angiotensin II induced cardiovascular remodeling and renal insufficiency. Circ Res. 2008; 102:68–76. [PubMed: 17967781]
16. Delbosc S, Cristol JP, Descomps B, Mimran A, Jover B. Simvastatin prevents angiotensin II-induced cardiac alteration and oxidative stress. Hypertension. 2002; 40:142–147. [PubMed: 12154104]
17. Node K, Fujita M, Kitakaze M, Hori M, Liao JK. Short-term statin therapy improves cardiac function and symptoms in patients with idiopathic dilated cardiomyopathy. Circulation. 2003; 108:839–843. [PubMed: 12885745]
18. Markle RA, Han J, Summers BD, Yokoyama T, Hajjar KA, Hajjar DP, et al. Pitavastatin alters the expression of thrombotic and fibrinolytic proteins in human vascular cells. J Cell Biochem. 2003; 90:23–32. [PubMed: 12938153]
19. Masamura K, Oida K, Kanehara H, Suzuki J, Horie S, Ishii H, et al. Pitavastatin-induced thrombomodulin expression by endothelial cells acts via inhibition of small G proteins of the Rho family. Arterioscler Thromb Vasc Biol. 2003; 23:512–517. [PubMed: 12615662]
20. Shibata S, Nagase M, Yoshida S, Kawarazaki W, Kurihara H, Tanaka H, et al. Modification of mineralocorticoid receptor function by Rac1 GTPase: implication in proteinuric kidney disease. Nat Med. 2008; 14:1370–1376. [PubMed: 19029984]
21. Cheng XW, Obata K, Kuzuya M, Izawa H, Nakamura K, Asahi E, et al. An elastolytic cathepsin induction/activation system exists in the rat and human myocardium and is upregulated in hypertensive heart failure. Hypertension. 2006; 48:979–987. [PubMed: 16982960]
22. Nagase M, Shibata S, Yoshida S, Nagase T, Gotoda T, Fujita T. Podocyte injury underlies the glomerulopathy of Dahl salt-hypertensive rats and is reversed by aldosterone blocker. Hypertension. 2006; 47:1084–1093. [PubMed: 16636193]
23. Saka M, Obata K, Ichihara S, Cheng XW, Kimata H, Nishizawa T, et al. Pitavastatin improves cardiac function and survival in association with suppression of the myocardial endothelin system in a rat model of hypertensive heart failure. J Cardiovasc Pharmacol. 2006; 47:770–779. [PubMed: 16810078]
24. Doublier S, Salvidio G, Lupia E, Ruotsalainen V, Verzola D, Deferrari G, et al. Nephrin expression is reduced in human diabetic nephropathy: evidence for a distinct role for glycated albumin and angiotensin II. Diabetes. 2003; 52:1023–1030. [PubMed: 12663475]
25. Ichihara S, Noda A, Nagata K, Obata K, Xu J, Ichihara G, et al. Pravastatin increases survival and suppresses an increase in myocardial matrix metalloproteinase activity in a rat model of heart failure. Cardiovasc Res. 2006; 69:726–735. [PubMed: 16165109]
26. Jaffe IZ, Mendelsohn ME. Angiotensin II and aldosterone regulate gene transcription via functional mineralocortocoid receptors in human coronary artery smooth muscle cells. Circ Res. 2005; 96:643–650. [PubMed: 15718497]
27. Behr TM, Wang X, Aiyar N, Coatney RW, Li X, Koster P, et al. Monocyte chemoattractant protein-1 is upregulated in rats with volume-overload congestive heart failure. Circulation. 2000; 102:1315–1322. [PubMed: 10982549]

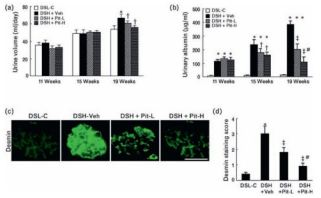

Fig. 1.

Urine volume and urinary albumin in the four experimental groups. Temporal profiles of (a) urine volume and (b) urinary albumin in the control (DSL-L), vehicle (DSH+Veh), low-dose pitavastatin (DSH+Pit-L), and high-dose pitavastatin (DSH+Pit-H) groups at the three indicated time points (n = 10 in each group). (c) Representative images of immunostaining and (d) combined quantitative data for desmin staining score at 20 weeks of age are shown. DSH, Dahl rat fed high salt (8%, DSH); DSL, Dahl rat fed low salt (0.3%, DSL). Scale bar = 100 μm. Values are means ± SEM (n = 6). *P <0.05 vs. corresponding control at 11, 15, or 19 weeks of age; $^{\dagger}P$ <0.05, $^{\ddagger}P$ <0.01 vs. DSH-Veh at 15 or 19 weeks of age; $^{\#}P$ <0.05 vs. DSH+Pit-L at 19 weeks of age.

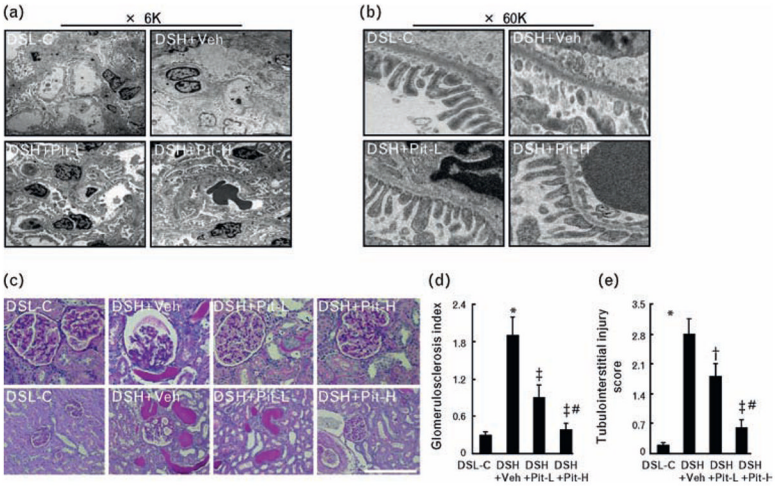

Fig. 2.

Effects of pitavastatin on glomerular and podocyte injuries on the kidneys of DSH rats at 20 weeks of age. Representative transmission electron microscopy (TEM) images at ×6000 (a, left; 6K) and ×60 000 (b, right; 60K). (c) Representative micrographs of periodic acid-Schiff-stained renal sections from DSL-C, DSH+Veh, DSH+Pit-L, and DSH+Pit-H rats. Scale bar = 100 μm. (d) Glomerulosclerosis index. (e) Tubulointerstitial injury score. DSH, Dahl rat fed high salt (8%, DSH); DSL, Dahl rat fed low salt (0.3%, DSL). Values are means ± SEM (n = 6). Values are means ± SEM. *P <0.05 vs. DSL-C; $^{\dagger}P$ <0.05, $^{\ddagger}P$ <0.01 vs. DSH+Veh; $^{\#}P$ <0.05 vs. DSH+Pit-L. Scale bars = 100 μm.

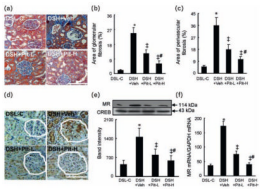

Fig. 3.

Glomerular and perivascular fibrosis and mineralocorticoid receptor gene expression in the four experimental groups at 20 weeks of age. (a) Representative images of azan Mallory-stained renal sections from DSL-C, DSH+Veh, DSH+Pit-L, and DSH+Pit-H rats. (b) and (c) Areas of glomerular and perivascular fibrosis, respectively. (d) Representative images of immunostaining for mineralocorticoid receptor. White outlines indicate glomeruli. (e) and (f) Quantitative analysis of western blot for mineralocorticoid receptor protein production (n = 6). (e) Real-time PCR for mineralocorticoid receptor mRNA expression (n = 8). (f) Values are means ± SEM. P <0.05 vs. DSL-C; $^{\ddagger}P$ <0.01 vs. DSH+Veh; $^{\#}P$ <0.05 vs. DSH+Pit-L. DSH, Dahl rat fed high salt (8%, DSH); DSL, Dahl rat fed low salt (0.3%, DSL). Scale bars = 100 μm.

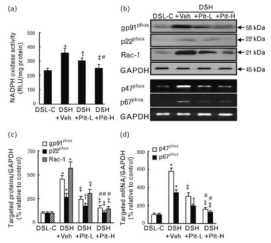

Fig. 4.

The levels of nicotinamide-adenine dinucleotide phosphate oxidase activity and nicotinamide-adenine dinucleotide phosphate oxidase subunit mRNAs and/or proteins in the four groups at 20 weeks of age. (a) Quantitative analysis of nicotinamide-adenine dinucleotide phosphate (NADPH) oxidase activity ($n = 8$). (b) Representative images of western blot and PCR blots for NADPH oxidase subunits. (c) and (d) Quantification of the data for the levels of $gp91^{phox}$ and $p22^{phox}$ and Rac-1 proteins (c) and $p47^{phox}$ $p67^{phox}$ mRNAs (d) is shown; band intensity was normalized to that for glyceraldehyde 3-phosphate dehydrogenase (GAPDH; $n = 6$). Values are means ± SEM. $^{*}P < 0.05$ vs. DSL-C; $^{\dagger}P < 0.05$, $^{\ddagger}P < 0.01$ vs. DSH+Veh; $^{\#}P < 0.05$ vs. DSH+Pit-L. DSH, Dahl rat fed high salt (8%, DSH); DSL, Dahl rat fed low salt (0.3%, DSL).

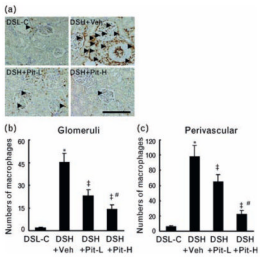

Fig. 5.

Macrophage staining in the four experimental groups at 20 weeks of age. (a–c) Representative images of immunostaining (a) and combined quantitative data for macrophage infiltration in (b) glomeruli and (c) perivascular regions in DSL-C, DSH-Veh, DSH+Pit-L, and DSH+Pit-H rats. Arrowheads indicate infiltrated macrophages. DSH, Dahl rat fed high salt (8%, DSH); DSL, Dahl rat fed low salt (0.3%, DSL). Values are means ± SEM (n = 6). *P <0.05 vs. DSL-C; ‡P <0.01 vs. DSH+Veh; #P <0.05 vs. DSH+Pit-L. Scale bars = 100 μm.

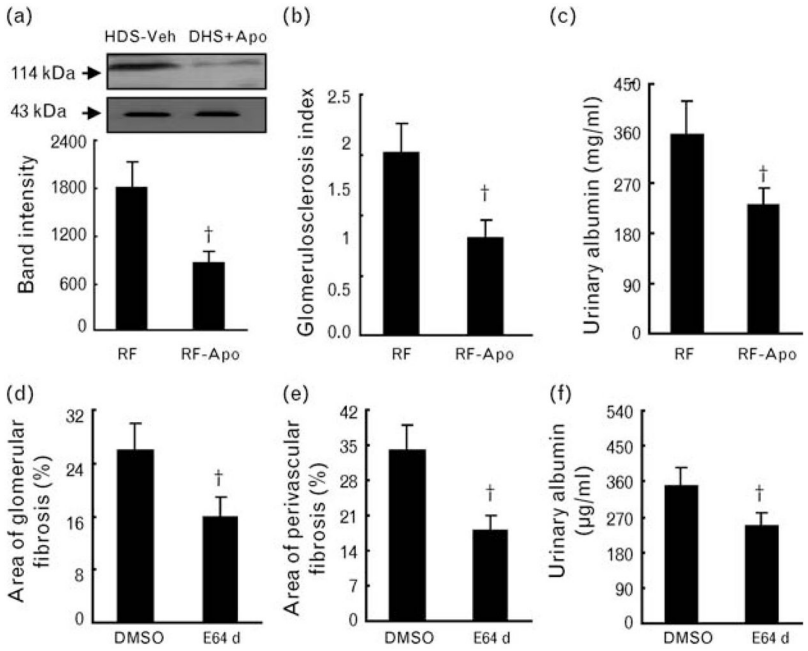

Fig. 6.

Effects of apocynin and E64d on mineralocorticoid receptor expression, glomerulosclerosis and urinary albumin. (a) Representative images of western blots and combined quantitative data for mineralocorticoid receptor protein production are shown; band intensity was normalized to that for the nuclear protein cyclic AMP response element-binding protein (CREB; $n = 6$). (b) and (c) Apocynin reduced the glomerulosclerosis index (b, $n = 6$) and urinary albumin (c, $n = 6$). (d–f) E64d lessened glomerular (d) and perivascular (e) fibrosis and urinary albumin (f). DSH, Dahl rat fed high salt (8%, DSH); DSL, Dahl rat fed low salt (0.3%, DSL). Values are means ± SEM. *P <0.05 vs. RF or E64d.

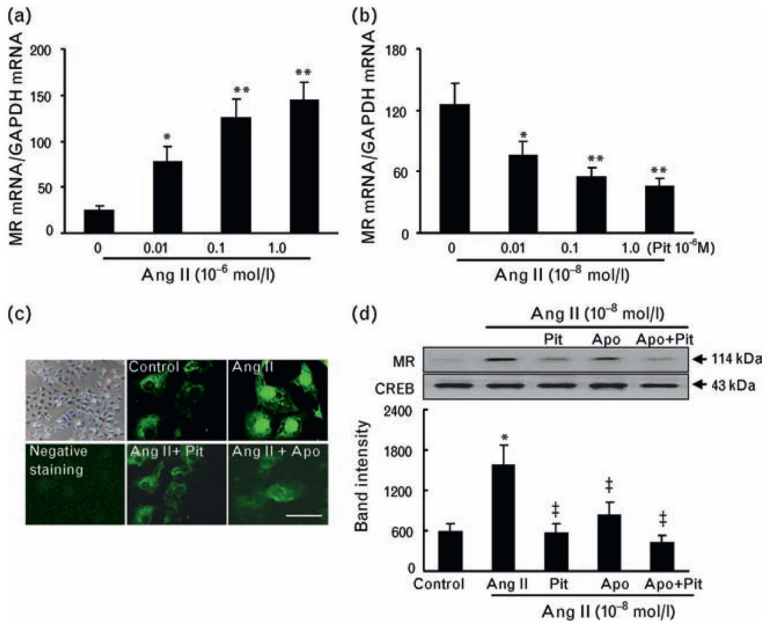

Fig. 7.

Regulation of mineralocorticoid receptor expression in cultured podocytes. (a) Angiotensin II (Ang II) stimulated mineralocorticoid receptor mRNA expression in a dose-dependent manner. (b) Following pretreatment with or without pitavastatin (Pit) at the indicated concentrations for 30 min, the podocytes were incubated with Ang II (0.1 μmol/l) for 24 h and subjected to quantitative real-time PCR analysis of mineralocorticoid receptor mRNA (n = 6). (c and d) Following pretreatment with or without apocynin (Apo) or Pit at the indicated concentrations for 30 min, the podocytes were incubated with Ang II (0.1 μmol/l) for 24 h and subjected to immunofluorescence and western blotting assays (n = 4) for mineralocorticoid receptor protein. DSH, Dahl rat fed high salt (8%, DSH); DSL, Dahl rat fed low salt (0.3%, DSL); RF, real failure. Values are means ± SEM. *P <0.05, **P <0.05 vs. corresponding control; ‡P <0.01 vs. Ang II alone.

Table 1

Levels of targeted genes and cytokine proteins in the kidneys or plasma of Dahl salt-sensitive rats

Gene	DHL-C	DHS+Veh	DHS+Pit-L	DHS+Pit-H
ELISA				
TNF-α (pg/ml)	2.5 ± 0.5	6.3 ± 1.5*	3.7 ± 1.3†	3.3 ± 1.5†
IL-1β (pg/ml)	10.1 ± 2.0	30.7 ± 3.4*	19.0 ± 3.3†	13.0 ± 3.1‡
Real-time PCR				
ACE	4.5 ± 0.9	8.5 ± 2.5*	6.1 ± 2.6†	3.5 ± 2.1‡,§
AT1R	56.2 ± 6.1	234.0 ± 17.8*	178.0 ± 11.4†	98.2 ± 9.3‡
MCP-1	45.0 ± 4.3	315.1 ± 35.5*	67.1 ± 14.7‡	22.4 ± 8.1‡,§
Osteopontin	23.0 ± 4.0	344.9 ± 45.2*	205.9 ± 84.2†	39.4 ± 9.3‡,§
Cathepsin S	31.0 ± 3.1	156.2 ± 18.4*	73.0 ± 10.1‡	40.4 ± 9.6‡,§
Cathepsin K	89.1 ± 7.2	101.8 ± 21.4	97.0 ± 34.0	80.0 ± 19.1
Cystatin C	56.2 ± 5.5	110.5 ± 20.5*	62.1 ± 10.0†	69.2 ± 18.1†
Cathepsin B	89.8 ± 10.0	177.6 ± 30.9*	124.8 ± 17.0†	121.3 ± 31.2†
Cathepsin L	67.3 ± 9.1	157.1 ± 33.2*	90.4 ± 12.6†	69.6 ± 14.7†
Type I collagen	34.0 ± 4.3	158.1 ± 34.1*	45.0 ± 10.2‡	18.6 ± 9.0‡,§
Type III collagen	14.3 ± 2.0	36.3 ± 10.2*	21.1 ± 5.1†	6.5 ± 1.6‡,§

The levels of plasma tumor necrosis factor-α (TNF-α) and interleukin-1β (IL-1β) were analyzed with ELISA kits. The mRNA levels of the indicated genes in the kidney tissues of four groups of Dahl salt-sensitive rats were quantified by real-time PCR. PCR data were normalized to the abundance of glyceraldehyde 3-phosphate dehydrogenase (GAPDH) mRNA. Data are means ± SEM (n = 8). ACE, angiotensin-converting enzyme; AT1R, angiotensin II type 1 receptor; MCP, monocyte chemoattractant protein.

*P <0.05 vs. DHS-C.

†P <0.05.

‡P <0.01 vs. DHS+Veh.

§P <0.05 vs. Pit-L.